

**EXCLUSIVE PHOTON-INDUCED HADRONIC REACTIONS
AT LARGE MOMENTUM TRANSFERS ***

W.SCHWEIGER [†]

*Institute of Theoretical Physics, University of Graz, Universitätsplatz 5
A-8010 Graz, Austria*

ABSTRACT

It is generally assumed that due to factorization of long- and short-distance dynamics perturbative QCD can be applied to exclusive hadronic reactions at large momentum transfers. Within such a perturbative approach diquarks turn out to be a useful phenomenological device to model non-perturbative effects still observable in the kinematic range accessible by present-days experiments. The basic ingredients of the perturbative formalism with diquarks, i.e. Feynman rules for diquarks and quark-diquark wave functions of baryons, are briefly summarized. Applications of the diquark model to the electromagnetic form factors of the proton in the space- as well as time-like region, Compton-scattering off protons, $\gamma\gamma \rightarrow p\bar{p}$, and photoproduction of Kaons are discussed.

1. Introduction and Motivation

Despite the big progress achieved in strong-interaction physics since the advent of QCD, in particular in the understanding of deep inelastic scattering ¹, the appropriate theoretical description of **exclusive hadronic reactions** for momentum transfers reaching from a few GeV up to the highest values accessible by present-days experiments remains still a challenging problem. This is just the kinematic range where the transition from the non-perturbative to the perturbative regime of QCD is commonly believed to take place. Therefore the physical picture of such reactions is not as clear-cut as one may hope. The situation is reflected by the fact that some of the experimentally measured exclusive observables exhibit features typical for perturbative QCD already at a few GeV of momentum transfer, whereas others do not. Features characteristic for pQCD are in particular **suppression of hadronic helicity flips** ² and (fixed angle) **power laws** ³ obeyed by exclusive scattering amplitudes

*Talk given at the 7th Adriatic Meeting on Particle Physics, Brijuni (Croatia), September 1994

[†]E-mail: schweigerw@edvz.kfunigraz.ac.at

at large momentum transfer Q – in electron-proton scattering, e.g., the Dirac form factor F_1^p is expected to scale like Q^{-4} . Both these features are a consequence of the basic assumption entering the pQCD approach, namely **factorization of long- and short-distance dynamics** ^{4,5}.

According to the theoretical framework emerging from the factorization hypothesis, the so called “Hard Scattering Picture” (HSP), an exclusive hadronic amplitude T can be expressed as a convolution of process independent distribution amplitudes (DAs) ϕ_{H_i} with a perturbative hard amplitude \hat{T} for the scattering of collinear constituents

$$T = \int_0^1 \hat{T}(x_j, Q) \prod_{H_i} \left(\phi_{H_i}(x_j, \tilde{Q}) \delta\left(1 - \sum_{k=1}^{n_i} x_k\right) \prod_{j=1}^{n_i} dx_j \right). \quad (1)$$

To leading order in $(1/Q)$ only tree-graphs, obtained by replacing each of the external hadrons by its valence Fock state, contribute to \hat{T} . The distribution amplitudes ϕ_{H_i} are probability amplitudes for finding the pertinent valence Fock-state in the hadron H_i with the constituents carrying the longitudinal momentum fractions x_j of the parent hadron and being collinear up to the (factorization) scale \tilde{Q} .

As a simple illustration for the apparent successes and also the limitations of the HSP let me mention (once more) the electromagnetic form factors of the proton:

- on the one hand, the data for the helicity-non-flip Dirac form factor F_1^p indeed seem to scale according to perturbative QCD for $Q^2 \gtrsim 10 \text{ GeV}^2$ ⁶ (cf. Fig.1);
- on the other hand, the helicity-flip form factor F_2^p is still sizable around 10 GeV^2 , $(Q^2 F_2^p(Q^2)/F_1^p(Q^2))|_{Q^2=8.83 \text{ GeV}^2} = 1.143_{-0.403}^{+0.821} \text{ GeV}^2$ ⁷, violating helicity conservation. The pure quark HSP only states that F_2^p should be suppressed as compared to F_1^p by a factor \tilde{m}^2/Q^2 (where \tilde{m} is some soft scale) – the recent data on F_1^p and F_2^p indeed seem to confirm such a behaviour (cf. Fig. 2). However, the pure quark HSP cannot provide any quantitative predictions for F_2^p .

Also in other exclusive hadronic reactions, like elastic p-p scattering ⁸, violation of hadronic helicity conservation is observed which amounts up to $\approx 20 - 30\%$ even at a few GeV of momentum transfer. Among others these findings can be regarded as a hint that soft contributions not accounted for by the pure quark HSP are still present in the few-GeV region.

In order to cope with such effects a phenomenological model has been proposed in a series of papers ^{9,10,11,12} which still pursues the perturbative approach, in which baryons, however, are treated as quark-diquark systems. This picture is primarily motivated by the observation that most of the octet-baryon DAs derived via QCD sum-rules (at finite \tilde{Q}) are very asymmetric ¹³, indicating strong quark-quark correlations. Actually, a very asymmetric DA, which strongly favours the helicity-parallel u quark, is needed for the proton to achieve a quantitative description of F_1^p for $Q^2 \gtrsim 10 \text{ GeV}^2$ ¹⁴. For the completely symmetric DA $\propto x_1 x_2 x_3$, which emerges in the limit $\tilde{Q} \rightarrow \infty$, the form factor F_1^p becomes identically zero.

2. The Hard-Scattering Picture with Diquarks

As has been mentioned already, there are two elements entering the calculation of an exclusive amplitude within the HSP, namely a hard scattering amplitude \hat{T} , to be calculated in collinear approximation within perturbative QCD, and DAs ϕ . To leading order in $1/Q$ the scattering amplitude is determined by the valence Fock states of the hadrons under consideration – in the diquark model a **quark-diquark** state in case of an ordinary baryon. If one assumes the diquark to be in its ground state it can be either a spin 0 (scalar) diquark or a spin 1 (axial vector) diquark. The introduction of vector diquarks occurs to be essential if one wants to describe spin effects. By the way, there are many fields of hadronic physics, like baryon spectroscopy, deep inelastic scattering, or weak decays, to mention a few, in which the concept of diquarks has already been applied successfully. Recently, a comprehensive review of the main ideas about diquarks has been published by M. Anselmino et al. ¹⁵.

To come back to exclusive scattering, let us continue with baryon wave functions in terms of the quark and diquark constituents. For the lowest lying baryon octet, assuming zero relative orbital angular momentum between quark and diquark the wave functions (already integrated over transverse momenta) can be cast into the form

$$|B; p, \lambda\rangle = f_S \phi_S^B(x_1) \chi_S^B u(p, \lambda) + (f_V/\sqrt{3}) \phi_V^B(x_1) \chi_V^B (\gamma^\alpha + p^\alpha/m_B) \gamma_5 u(p, \lambda). \quad (2)$$

The two terms in Eq.(2) represent configurations consisting of a quark and either a scalar (S) or vector (V) diquark. Thereby advantage has been taken of the collinear situation, $p_q = x_1 p$ and $p_D = x_2 p = (1 - x_1)p$ (x_1 is the longitudinal momentum fraction of the quark) to rewrite the spin part of the wave function in a covariant way. The pleasant feature of the wave-function representation Eq.(2) is that it contains, besides x_1 , only baryonic quantities (momentum p , helicity λ , baryon mass m_B).

For an SU(6)-like spin-flavour dependence, which means starting from the SU(6) wave function for three quarks and combining, let us say, quark 2 and 3 to a diquark, the flavour functions χ for proton and, e.g., Λ take on the form

$$\chi_S^p = uS_{[u,d]}, \quad \chi_V^p = [uV_{\{u,d\}} - \sqrt{2}dV_{\{u,u\}}]/\sqrt{3}, \quad (3)$$

$$\chi_S^{\Lambda^0} = [uS_{[d,s]} - dS_{[u,s]} - 2sS_{[u,d]}]/\sqrt{6}, \quad \chi_V^{\Lambda^0} = [uV_{\{d,s\}} - dV_{\{u,s\}}]/\sqrt{2}. \quad (4)$$

The DAs $\phi_S^B(x_1)$ and $\phi_V^B(x_1)$ in Eq.(2) are nothing else but quark-diquark light-cone wave functions integrated over the transverse momentum. f_S and f_V are the $r = 0$ values of the corresponding configuration space wave functions. Since the model is applied to a very restricted momentum-transfer range ($3 - 30 \text{ GeV}^2$) the QCD evolution of these DAs, which brings in only a weak logarithmic \bar{Q} dependence, is neglected. In general, very little is known on the shape of quark-diquark DAs. Hence one is forced to make a phenomenological ansatz for which an expression of the form

$$\phi_D^B(x_1) = N_D x_1 x_2^3 (1 + c_{1D} x_1 + c_{2D} x_1^2) \exp \left[-b^2 \left(m_q^2/x_1 + m_D^2/x_2 \right) \right], \quad (5)$$

where D can be either S or V , proves to be quite appropriate. Actually, the constants c_{1S} and c_{2S} are fixed to zero. For $c_{1D} = c_{2D} = 0$ the form of the DA (5) can be traced back to a nonrelativistic harmonic-oscillator wave function¹⁶. Therefore the masses appearing in the exponentials have to be considered as constituent masses (330 MeV for light quarks, 580 MeV for light diquarks, strange quarks are 150 MeV heavier than light quarks). The oscillator parameter $b^2 = 0.248\text{GeV}^{-2}$ is chosen in such a way that the full wave function gives rise to a value of 600 MeV for the mean intrinsic transverse momentum of quarks inside a nucleon. The “normalization constants” N_S and N_V are determined by the condition $\int_0^1 dx_1 \phi_{S(V)}(x_1) = 1$.

Concerning colour, the diquark behaves like an antiquark. In order to give a colourless baryon in combination with a colour triplet quark the diquark has to be in a colour antitriplet state.

The ingredients of the perturbative part of the model are gluon-diquark and photon-diquark vertices which are introduced following the standard prescriptions for the coupling of a spin-1 gauge boson to a spin-0 or a spin-1 particle, respectively¹¹. Thereby V diquarks are allowed to possess an anomalous (chromo)magnetic moment κ_V . In applications of the model Feynman graphs are calculated first with these Feynman rules for point-like diquarks. In order to take into account the composite nature of diquarks the n -point contributions, i.e. those Feynman graphs where $n - 2$ gauge bosons couple to the diquark, are multiplied afterwards with phenomenological vertex functions – diquark form factors. The particular choice

$$F_S^{(3)}(Q^2) = \delta_S Q_S^2 / (Q_S^2 + Q^2), \quad F_V^{(3)}(Q^2) = \delta_V \left(Q_V^2 / (Q_V^2 + Q^2) \right)^2 \quad (6)$$

for 3-point functions and

$$F_S^{(n)} = a_S F_S^{(3)}(Q^2), \quad F_V^{(n)} = a_V F_V^{(3)}(Q^2) \left(Q_V^2 / (Q_V^2 + Q^2) \right)^{(n-3)} \quad (7)$$

for n -point functions ($n \geq 4$) ensures that in the limit $Q^2 \rightarrow \infty$ the scaling behaviour of the diquark model goes over in that of the pure quark HSP. If one knew the quark-quark distribution amplitude of a diquark one could in principle calculate these form factors from the pure quark HSP. The factor $\delta_{S(V)} = \alpha_s(Q^2) / \alpha_s(Q_{S(V)}^2)$ ($\delta_{S(V)} = 1$ for $Q^2 \leq Q_{S(V)}^2$) provides the correct powers of $\alpha_s(Q^2)$ for asymptotically large Q^2 . For the running coupling α_S the one-loop result $\alpha_S = 12\pi/25 \ln(Q^2/\Lambda_{QCD}^2)$ is used with $\Lambda_{QCD} = 200\text{MeV}$. In addition α_S is restricted to be smaller than 0.5. a_S and a_V are strength parameters which allow for the possibility of diquark excitation and break-up in intermediate states where diquarks can be far off-shell.

3. Parameter Fixing and Electromagnetic Form Factors of the Proton¹¹

The open parameters of the model are the cut-off masses Q_S^2 and Q_V^2 occurring in the diquark form factors, the anomalous (chromo)magnetic moment of the vector diquark κ_V , the strength parameters of the n -point functions a_S and a_V , and the parameters in the diquark DAs f_S , f_V , c_{1V} , and c_{2V} . These parameters have been

Fig. 1. The magnetic form factor of the proton in the space-like and time-like ($s = -Q^2$) regions. The solid lines represent the corresponding predictions of the diquark model. The space-like data are taken from Sill et al. ⁶(●), the time-like data are taken from Bardin et al. ²²(+), Antonelli et al. ²³(□), and Armstrong et al. ¹⁹(○).

determined by means of e-p and e-n scattering data in the range $3 \text{ GeV}^2 \lesssim Q^2 \lesssim 30 \text{ GeV}^2$, namely $(d\sigma/d\Omega)_{ep}$ ⁶, G_E^p and G_M^p ⁷ (extracted via Rosenbluth separation), σ_n/σ_p ¹⁷, G_E^n and G_M^n ¹⁸.

A good fit to the data is accomplished with the parameter set

$$\begin{aligned} f_S &= 73.85\text{MeV}, \quad Q_S^2 = 3.22\text{GeV}^2, \quad a_S = 0.15, \\ f_V &= 127.7\text{MeV}, \quad Q_V^2 = 1.50\text{GeV}^2, \quad a_V = 0.05, \quad \kappa_V = 1.39, \quad c_1 = 5.8, \quad c_2 = -12.5. \end{aligned} \quad (8)$$

The results for the proton magnetic form factor G_M^p and the Pauli form factor F_2^p are depicted in Figs. 1 and 2, respectively. It should be emphasized that unlike the pure quark HSP, which cannot make any quantitative predictions for the helicity-flip Pauli form factor F_2^p , the diquark model provides reasonable results also for this quantity.

After having fixed the parameters of the diquark model by means of elastic e-N scattering we are now in the position to see how it works for other exclusive reactions.

4. Applications of the Diquark Model

4.1. Proton Magnetic Form Factor in the Timelike Region ¹²

The nearest application at hand is the continuation of the nucleon form factors to the timelike region, i.e. to consider in particular $e^+ e^- \rightarrow p \bar{p}$ or $p \bar{p} \rightarrow e^+ e^-$ scattering. These reactions are already a serious challenge for the pure quark HSP, which predicts $G_M^p(s) = G_M^p(Q^2 = -s)$. By way of contrast, recent measurements performed by the E760 collaboration at Fermilab ¹⁹ get results for the proton magnetic form factor in the timelike region which are more than 2 times larger than the spacelike values, even for $Q^2 \gtrsim 10 \text{ GeV}^2$. Thus it seems very hard for the pure quark HSP to

Fig. 2. The Pauli form factor of the proton F_p^2 scaled by Q^6 . The solid line represents the result obtained with the diquark model. Data are taken from Andivalis et al. ⁷ (●).

reconcile the space- and timelike predictions. Some improvement has been achieved by Hyer ²⁰, who took into account radiative (Sudakov) corrections, but a more or less sizable discrepancy – depending on the proton DA employed – is still observable.

Applying the diquark model to timelike processes requires some care with respect to the diquark form factors. One has to keep in mind that the multipole parameterization of the diquark form factors is only an effective description of the composite nature of diquarks. It is not possible to continue this parameterization in a unique way to the timelike region since the exact dynamics of the diquark system is not known. The simple analytic continuation $Q^2 \rightarrow -s$ indeed leads to poles in the diquark form factors which have no physical meaning. In order to avoid such unphysical poles the diquark form factors are kept constant once they reach a certain value, say c_0 , i.e.

$$F_D^{(n)}(s) = F_D^{(n)}(-Q^2), \quad s \geq s_0 \quad \text{and} \quad F_D^{(n)}(s) = c_0 = F_D^{(n)}(s_0), \quad s < s_0. \quad (9)$$

A similar recipe has also been used in a study of (inclusive) e^+e^- annihilation into hadrons ²¹. From Eq.(9) it is evident that the diquark form factors and hence also the proton magnetic form factor have larger values for a given s (> 0) than for the corresponding $Q^2 = -s$. In the timelike region one is closer to the form factor singularity than in the spacelike domain. This resembles the situation in the vector-meson dominance model.

c_0 is of course a new parameter of the model. But once it is fixed the diquark model should also be applicable to other timelike reactions. One finds good agreement with the E-760 data on G_M^p for $c_0 = 1.3$ (cf. Fig.1). As will be seen in Sect.4.3 this prescription also gives reasonable results for $\gamma\gamma \rightarrow p\bar{p}$.

Fig. 3. The Compton cross section vs. $\cos(\vartheta)$ for various photon lab. energies. Data are taken from Shupe et al. ²⁵. Solid line: diquark-model result at 4 GeV ($s = 8.4 \text{ GeV}^2$); dashed line: prediction of the pure quark HSP ²⁴.

4.2. Compton Scattering off Protons ¹⁰

For Compton scattering differential cross section data are available up to $|t| \approx 4\text{GeV}^2$. $\gamma p \rightarrow \gamma p$ is usually described by 6 independent (cms) helicity amplitudes

$$\begin{aligned}
 \phi_1 &= M_{1\frac{1}{2},1\frac{1}{2}} \sim s^{-2}, & \phi_2 &= M_{-1-\frac{1}{2},1\frac{1}{2}} \sim s^{-5/2}, \\
 \phi_3 &= M_{-1\frac{1}{2},1\frac{1}{2}} \sim s^{-3}, & \phi_4 &= M_{1-\frac{1}{2},1\frac{1}{2}} \sim s^{-5/2}, \\
 \phi_5 &= M_{1-\frac{1}{2},1-\frac{1}{2}} \sim s^{-2}, & \phi_6 &= M_{-1\frac{1}{2},1-\frac{1}{2}} \sim s^{-5/2}.
 \end{aligned} \tag{10}$$

In Eq.(10) the (fixed angle) large s behaviour of the helicity amplitudes, as resulting from the diquark model, is already indicated. ϕ_1 , ϕ_3 and ϕ_5 conserve the helicity of the proton, whereas the others do not.

A new interesting feature showing up in Compton scattering is the occurrence of a relative phase between helicity flip and non-flip amplitudes. This comes about because in diagrams where the two photons couple to different constituents (4-point contributions) the exchanged gluon goes on-shell within the range of x -integration. Such a situation occurs in the pure quark HSP as well. The usual treatment of the propagator poles $(g^2 \pm i\epsilon)^{-1} = \mathcal{P}(g^{-2}) \mp i\pi\delta(g^2)$ then leads to an imaginary part for the corresponding amplitudes. Together with non-vanishing helicity-flip amplitudes (generated by the vector diquarks) this gives rise to a transverse polarization.

In Fig.3 the diquark model result is confronted with experiment. Also plotted is a prediction of the pure quark HSP for the Chernyak-Ogloblin-Zhitnitsky DA ²⁴.

Fig. 4. The integrated cross-section ($|\cos(\theta)| \leq 0.6$) for $\gamma\gamma \rightarrow p\bar{p}$ as a function of \sqrt{s} as resulting from the diquark model. Data are taken from Artuso et al. ²⁶.

4.3. $\gamma\gamma \rightarrow p\bar{p}$ ¹²

Simultaneously with Compton scattering also the crossed process $\gamma\gamma \rightarrow p\bar{p}$ has been considered. Unlike Compton scattering there occur no propagator singularities since Mandelstam s and t are now interchanged. Shown in Fig.4 is the integrated cross-section ($|\cos\theta| \leq 0.6$) for two-photon annihilation into $p\bar{p}$ as a function of \sqrt{s} . For $\sqrt{s} \gtrsim 2.5$ GeV good agreement with the recent CLEO data ²⁶ can be observed. The pure quark model results of Farrar et al. ²⁷ lie down by about a factor of 8. Similar to the magnetic form factor of the proton in the timelike region radiative (Sudakov) corrections have also been found to improve the situation in two-photon annihilation to a certain extend ²⁰.

4.4. Photoproduction of Kaons ³⁰

Photoproduction of mesons $\gamma p \rightarrow MB$ represents a large class of photon-induced reactions for which data at a few GeV of momentum transfer already exist ^{25,28}. Further data at even larger s , t , and u can be expected within the not-too-far future from the DESY e-p collider HERA. From the theoretical point of view, photoproduction means one step further in complexity as compared to Compton scattering. Within the diquark model the number of Feynman diagrams contributing is in general nearly three times larger (158) than for $\gamma p \rightarrow \gamma p$ (64). However, there are fortunately a few photoproduction reactions for which matters become somewhat simpler - namely those where the baryon B in the final state is a Λ . Since the p and the Λ have in common only the $S(u)$ diquark such processes proceed solely through the S diquark. For an analogous reason only V diquarks are involved if the baryon becomes a Σ^0 . Since $\gamma p \rightarrow K^+\Lambda$ only proceeds via S diquarks, scattering amplitudes and hence observables which require a flip of the baryonic helicity (like the proton asymmetry or

Fig. 5. The photoproduction cross section vs. $\cos\theta$ for $\gamma p \rightarrow K^+\Lambda$. The solid line represents the diquark-model result for the p and Λ DA of Eq.(5) and the K^+ DA of Eq.(12). The dashed line represents a result obtained within the pure quark HSP²⁹. Data are taken from Ref.[25]

the Lambda polarization) become zero. Photoproduction of pseudoscalar mesons in general can be described by 4 independent helicity amplitudes

$$N = M_{-\frac{1}{2},1\frac{1}{2}}, \quad S_1 = M_{-\frac{1}{2},1-\frac{1}{2}}, \quad D = M_{\frac{1}{2},1-\frac{1}{2}}, \quad S_2 = M_{\frac{1}{2},1\frac{1}{2}}. \quad (11)$$

Since only scalar diquarks take part in $\gamma p \rightarrow K^+\Lambda$ two of the 4 helicity amplitudes vanish, $N = D = 0$. The remaining two amplitudes, S_1 and S_2 , scale asymptotically like $s^{-5/2}$ and hence for large s the differential cross section should decrease $\propto s^{-7}$.

The hard scattering amplitude \hat{T} for $\gamma p \rightarrow K^+\Lambda$ is given by all tree graphs for $\gamma u S(ud) \rightarrow u \bar{s} s S(ud)$, altogether 63. As in Compton scattering one encounters propagator singularities which give rise to an imaginary part in the helicity amplitudes. A new feature, however, showing up in photoproduction is the occurrence of triple gluon vertices.

With the Λ DA given in Eq.(5) (note, that this DA already contains a flavour dependence due to the constituent masses m_q and m_D), an analogous form for the K^+ DA

$$\phi^{K^+}(x_1) \propto x_1(1-x_1) \exp\left[-b^2\left(m_u^2/x_1 + m_s^2/(1-x_1)\right)\right], \quad (12)$$

and f_K fixed according to the experimental relation between K and π decay constants, $f_K = 1.2f_\pi$, reasonable agreement with the data can be achieved already without introducing additional parameters (cf. Fig.5). The predictions of the pure quark HSP, also plotted in the figure, have been obtained with very asymmetric DAs for all hadrons involved. With the double humped Kaon DA used by these authors the diquark-model result can even be improved.

5. Outlook and Conclusions

For a phenomenological model, like the diquark model, it is certainly necessary to calculate as many reactions as possible in a consistent way to check its usefulness. For the simplest electron and photon-induced reactions (form factors, Compton scattering, electroproduction of Kaons, ...) it already seems to work reasonably well. Presently, the photoproduction of arbitrary mesons, which requires the calculation of Feynman diagrams not only for scalar, but also for vector diquarks, is under investigation. Unfortunately, exclusive data in the few-GeV region are often of poor quality and are mostly restricted to spin-averaged quantities. Spin observables would set, of course, the most stringent constraints. However, with the increasing number of reactions considered and with more and better exclusive data from new facilities like CEBAF it will undoubtedly be possible to clarify the role which diquarks play in exclusive scattering.

6. Acknowledgement

Most of the results presented in this contribution are the outcome of a close collaboration with R.Jakob, P.Kroll, M.Schürmann (University of Wuppertal, FRG) and K.Pasek (Rudjer Bošković Institute Zagreb, Croatia). I would like to thank them for many fruitful discussions and suggestions.

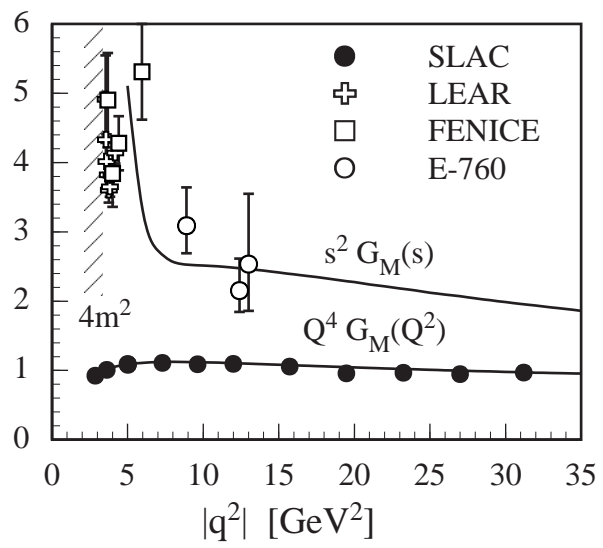
7. References

1. W.J.Stirling, in *Substructures of Matter as Revealed with Electroweak Probes*, eds. L.Mathelitsch and W.Plessas (Springer, Berlin-Heidelberg, 1994) 121.
2. S.J.Brodsky and G.P.Lepage, *Phys. Rev.* **D24** (1981) 2848.
3. S.J.Brodsky and G.R.Farrar, *Phys. Rev.* **D11** (1975) 1309.
4. G.P.Lepage and S.J.Brodsky, *Phys. Rev.* **D22** (1980) 2157.
5. A.V.Efremov and A.V.Radyushkin, *Phys. Lett.* **B94** (1980) 245.
6. A.F.Sill et al., *Phys. Rev.* **D48** (1993) 29.
7. L.Andivalis et al., *Phys. Rev.* **D50** (1994) 5491.
8. W.A.Crabb et al., *Phys. Rev. Lett.* **65** (1990) 3241.
9. P.Kroll, M.Schürmann, and W.Schweiger, *Z. Phys.* **A338** (1991) 339.
10. P.Kroll, M.Schürmann, and W.Schweiger, *Int. J. Mod. Phys.* **A6** (1991) 4107.
11. R.Jakob, P.Kroll, M.Schürmann, and W.Schweiger, *Z. Phys.* **A347** (1993) 109.
12. P.Kroll, Th.Pilsner, M.Schürmann, and W.Schweiger, *Phys. Lett* **B316** (1993) 546.
13. V.L.Chernyak, A.A.Ogloblin, and I.R.Zhitnitsky, *Z. Phys.* **A42** (1989) 569.
14. N.G.Stefanis, *Phys. Rev.* **D40** (1989) 2305.
15. M.Anselmino et al., *Rev. Mod. Phys.* **65** (1993) 1199.
16. T.Huang, *Nucl. Phys. [Proc. Suppl.]* **B7** (1989) 320.
17. S.Rock et al., *Phys. Rev.* **D46** (1992) 24.
18. A.Lung et al., *Phys. Rev. Lett.* **70** (1993) 718.

19. T.A.Armstrong et al., *Phys. Rev. Lett.* **70** (1993) 1212.
20. T.Hyer, *Phys. Rev.* **D47** (1993) 3875.
21. S.Ekelin et al., *Phys. Rev.* **D30** (1984) 2310.
22. G.Bardin et al., *Nucl. Phys.* **B411** (1994) 3.
23. A.Antonelli et al., *Phys. Lett.* **B334** (1994) 431.
24. A.S.Kronfeld and B.Nizic, *Phys. Rev.* **D44** (1991) 3445.
25. M.A.Shupe et al., *Phys. Rev.* **D19** (1979) 1921.
26. M.Artuso et al., *Phys. Rev.* **D50** (1994) 5484.
27. G.R.Farrar, E.Maina, and F.Neri, *Nucl. Phys.* **B259** (1985) 702; **B263** (1986) 746 (E).
28. R.L.Anderson et al., *Phys. Rev.* **D14** (1976) 679.
29. G.R.Farrar, K.Huleihel, and H.Zhang, *Nucl. Phys.* **B349** (1991) 655.
30. M.Schürmann, Thesis *WUB-DIS 92-4* (1992);
P.Kroll, K.Passek, M.Schürmann, and W.Schweiger: paper in preparation.

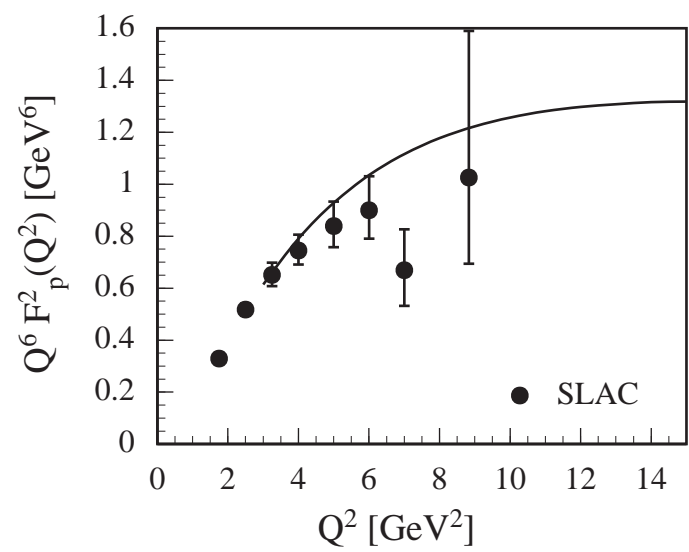
This figure "fig1-1.png" is available in "png" format from:

<http://arxiv.org/ps/hep-ph/9502208v1>



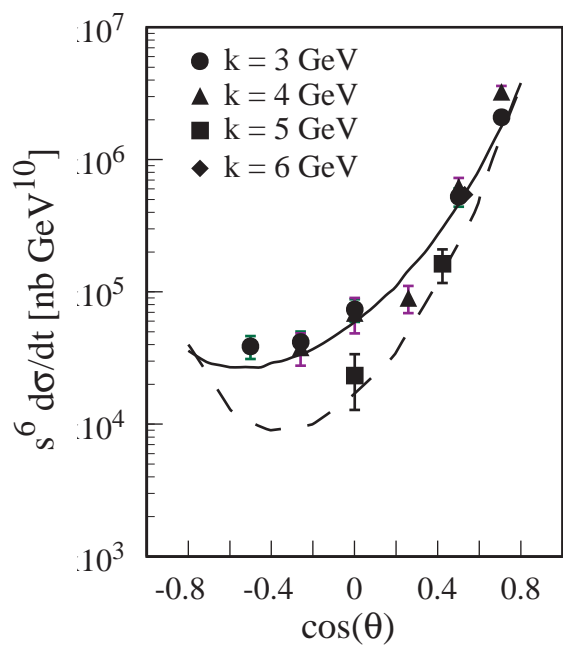
This figure "fig1-2.png" is available in "png" format from:

<http://arxiv.org/ps/hep-ph/9502208v1>



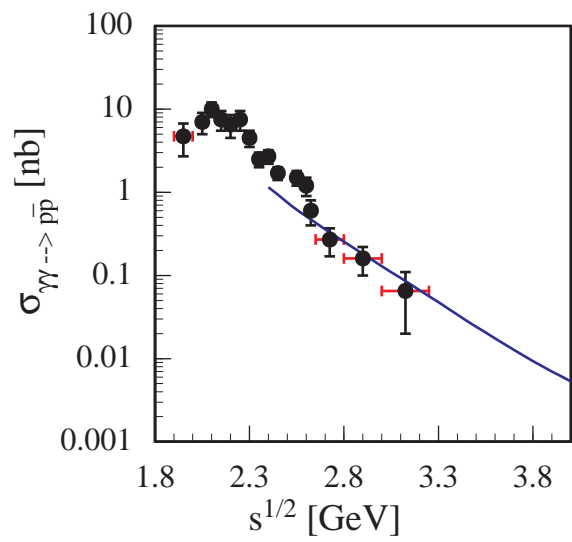
This figure "fig1-3.png" is available in "png" format from:

<http://arxiv.org/ps/hep-ph/9502208v1>



This figure "fig1-4.png" is available in "png" format from:

<http://arxiv.org/ps/hep-ph/9502208v1>



This figure "fig1-5.png" is available in "png" format from:

<http://arxiv.org/ps/hep-ph/9502208v1>

